ISSN 2004-2965 Energy Proceedings, Vol. 18, 2021

International Conference on Applied Energy 2021
Nov. 29 - Dec. 2, 2021, in Bangkok, Thailand
Paper ID: 112

Performance Evaluation of 33 kV Polymeric Outdoor Insulators Equipped with Non-Linear Field Grading Composites

M-Ramez Halloum [1*], Subba Reddy B. [1], G. Nithin Reddy [1]

Dept. of Electrical Engineering, Indian Institute of Science, Bengaluru, India.

ABSTRACT

This paper presents a study on 33 kV polymeric outdoor insulator's performance with non-linear resistive field grading composites based on Zinc Oxide microvaristors. The effect of non-linear field grading composites with optimized design and characteristics in stress control of 33 kV polymeric outdoor insulators using 2D models is evaluated. Also, a 3D model of the 33 kV polymeric insulator is developed to obtain more accurate and realistic results. The field computation and simulations are conducted using the (FEM) Finite Element Method and COMSOL Multiphysics. The proposed insulator with resistive field grading composite shows improved electric field distribution under various conditions. In addition, the heat generated along the insulator surface has been computed and compared. The simulation results demonstrate that the field grading of polymeric insulators using non-linear grading composites can improve the insulator performance under different surface conditions and increase the flashover voltage by reducing the potential of dry bands formation.

Keywords: polymeric outdoor insulator, non-linear resistive field grading composites, stress control, finite element method, ZnO microvaristors

NONMENCLATURE

Abbreviations	
ZnO	Zinc Oxide
FEM	Finite element method

1. INTRODUCTION

The usage of polymeric outdoor insulators in power systems is increasing remarkably for outdoor applications, mainly because of their superior characteristics compared with traditional insulation systems. One of the vital characteristics is the considerable weight reduction that may reach up to 90%. Also, superior mechanical strength and weight reduction decrease installation and maintenance costs and allow for long service life. In addition, the excellent hydrophobicity of silicone surfaces prevents the forming of the conductive film along the insulator surface in wet conditions and offers better performance under polluted conditions. Composite insulators are less vulnerable to severe damage from [1].

On the other hand, polymeric outdoor insulators have some limitations. They are more vulnerable to degradation and aging due to localized electric enhancements because of their organic nature. The electric field's distribution along the profile of polymeric insulators is highly non-homogeneous due to their structure, where the electric field is too high near both electrodes. These electric field enhancements may lead to premature degradation and erosion of polymeric materials. The performance of outdoor composite insulators is affected notably under wet-polluted conditions due to dry bands formation. These dry bands' arcs lead to early erosion and aging of materials [2].

Stress control and field grading in polymeric insulation systems is highly desired to alleviate such undesired consequences and ensure satisfying performance during service. Recently, many studies on various field grading composites to mitigate electric field stress in many HV equipment such as cable accessories, HV machinery, power electronics, and polymeric outdoor

Selection and peer-review under responsibility of the scientific committee of the 13th Int. Conf. on Applied Energy (ICAE2021).

insulators [3]-[7]. The latest advances in the ZnO microvaristors compounding process with silicone provide a promising solution to alleviate the localized enhancements in polymeric insulation systems [6]-[9].

In this paper, we proposed a suitable design and optimized switching parameters of field grading composite to control the electric stress of 33 kV polymeric insulators. COMSOL Multiphysics 5.5 with 2D axisymmetric and 3D models is adopted for the study. We assessed the new insulator with the optimized FGM under different conditions using 2D axisymmetric models. Further, we developed a 3D model to obtain a more accurate and realistic field distribution.

2. INSULATOR PROFILE AND COMPUTATION MODELS

Fig. 1. shows the 2D axisymmetric and the 3D models of the 33 kV polymeric outdoor insulator. The main structure of polymeric insulators comprises three main parts fiber core, insulation housing, and metallic end-fittings. The relative permittivity of the fiber core and silicone housing are 7.1 and 4.3, respectively. They have been assumed as perfect insulation materials with very low conductivity 1e-15 S/m. End-fittings are made of forged steel with a conductivity of 5.9e7 S/m. The wet pollution layer has been assumed to cover the insulator surface uniformly with a thickness of 0.5 mm. The relative permittivity and the conductivity of the wet pollution layer are 80 and 6e-7 S/m, respectively, and they have been adopted based on the results of laboratory experiments published in [10].

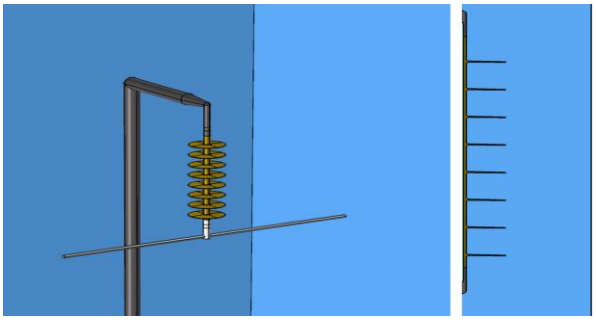

Fig. 1. The 2D axisymmetric and 3D model of the 33 kV polymeric outdoor insulator

The 2D axisymmetric model offers less memory size consumption and processing time. The insulator was surrounded by a large air region enough to not influence the field distribution around the insulator. Also, we developed A 3D model of the 33 kV polymeric outdoor insulator to consider the various structures around the insulator that affect the distribution of electric fields such as conductor and adjacent tower. The (RMS) applied voltage on the bottom electrode is 50 Hz, $33/\sqrt{3}$ kV, while the ground is connected to the top electrode. The mesh density was increased along the insulator surface.

We used the Electric Currents (ec) interface with a non-linear frequency solver, where inductive effects are negligible $\nabla \times \boldsymbol{E} = \frac{\partial \boldsymbol{B}}{\partial t} = 0$ where $\boldsymbol{E} = -\nabla V$ is the Electric field intensity, B is the magnetic flux density, and V is the electric potential [11]. The electric form of Gauss' law and the equation of continuity are given as follows: $\nabla . \boldsymbol{D} = \rho$ and $\nabla . \boldsymbol{J} = \nabla . \sigma \boldsymbol{E} = -j\omega\rho$.

Where $\boldsymbol{J} = \sigma \boldsymbol{E}$ is current density, $\boldsymbol{D} = \varepsilon_0 \varepsilon_r \boldsymbol{E}$ is electric flux density, ρ is the charge density, ε_0 is the vacuum permittivity, ε_r is the relative permittivity, and σ is the electrical conductivity. By combining both preceding equations, the software solves the following equation to obtain electric potential and field distribution: $-\nabla . (j\ \omega\ \varepsilon_0\ \varepsilon_r\ \nabla V) - \nabla . (\sigma\ \nabla V) = 0$.

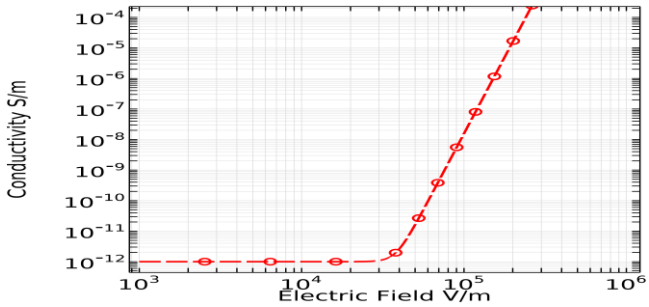

Fig. 2. Non-linear field-dependent conductivity of the nonlinear resistive FGM based on ZnO microvaristors

3. CHARACTERISTICS OF FIELD GRADING COMPOSITES BASED ON ZNO MICROVARISTORS

The latest advances in ZnO microvaristors manufacturing and compounding with silicone materials provide a promising solution to mitigate the electric enhancements in polymeric insulation systems. The non-linear characteristics of field grading materials can be obtained for many HV applications as required. Using different types of filler, filler concentration, size and shape of filler particles, and different insulating matrices, we can modify their non-linear properties over a wide range [6]-[9]. To initiate the gradient action of field grading composites, the filler concentration must be greater than the percolation threshold to form a continuous conduction path.

These new non-linear resistive field grading composites based on ZnO microvaristors are superior to the conventional field grading materials based on carbon black or silicon carbide (SiC). It has higher relative permittivity between 10 and 15; therefore, the refractive

effect will improve the overall field grading. In addition, power loss under normal operating conditions is less than conventional FGMs because of the lower initial conductivity [6]. Fig. 2. shows the non-linear conductivity of the field grading composite based on ZnO microvaristors used in this study. In the low field region, the field grading composite shows very low conductivity. Once the electric field intensity exceeded a particular value called field switching threshold (0.381e5 V/m), its conductivity highly increases to bring the critical regions to the conductive state, forming an opposite-field due to space charges formation. Thus, suppress the localized field enhancements in critical areas.

The relationship between the conductivity of field grading composite and electric field magnitude can be expressed by this exponential function as follows:

$$\sigma(E) = \sigma_0 \left[1 + \left(\frac{E}{E_b}\right)^{\alpha-1}\right]$$

Where σ_0 is the initial conductivity, E is the intensity of the electric field, E_b is the field switching threshold, and α is the nonlinearity coefficient. The relative permittivity of the field grading material is assigned as $\varepsilon_r = 12$ [3].

The switching characteristics of non-linear field grading composites have a vital role in obtaining effective field grading. The main parameter is the field switching threshold. To initiate its gradient action effectively, one must choose a suitable value within the electrical field ranges of the polymeric insulator. In contrast, choosing a very low value increases the resistive losses and transfers the stress to the end of the FGM layers. Also, a sufficiently high nonlinearity coefficient α is significantly required. The nonlinearity coefficient is practically between 10 and 20 because the advantage of a further increase is marginal. Furthermore, FGMs with higher nonlinearity coefficients required more complicated devices to manufacture [6].

Fig. 3. shows the distribution of electric field on the fiber core-silicone housing interface. The electric field distribution is highly non-homogeneous. It is too high near both electrodes; after about 50 mm it becomes more uniform. The field grading composites layers with a length of 50 mm and a thickness of 2 mm has been added on the fiber core-silicone housing interface and are covered with silicone rubber to protect them from various environmental stresses, as shown in Fig. 4. The optimized switching characteristics of FGMs were obtained using the 2D simulations as follows, $E_b = 0.381\text{e}5\ \text{V/m}$, $\alpha = 11$, and $\sigma_0 = 1e-12\ S/m$. These parameters offer the best performance beside terminals and toward the center area of the insulator and will be adopted for all coming simulations.

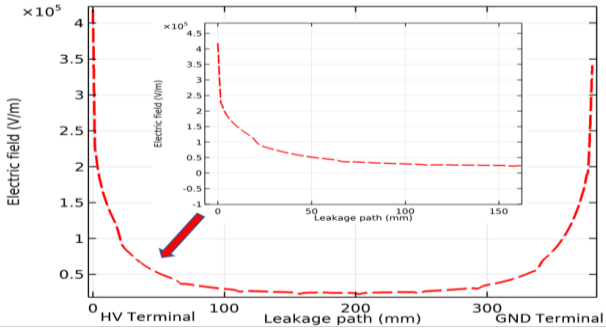

Fig. 3. Electric field distribution on the fiber core-silicone housing interface of polymeric outdoor insulator

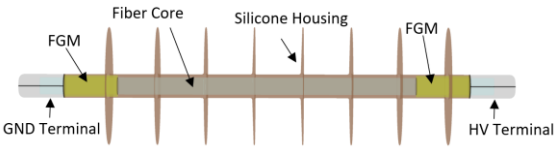

Fig. 4. Design of the polymeric outdoor insulator with non-linear field grading composites

4. SIMULATION RESULTS

4.1 Polymeric insulator performance with FGMs under dry and polluted conditions using 2D models

Fig. 5. and Fig. 6. show the tangential electric field distribution along the polymeric insulator profile under various surface conditions. As mentioned before, the electric field intensity under clean surface conditions is too high near both electrodes and gradually decreases towards the center. That is mainly because of the concentrated distribution of equipotential lines near both end-fittings and the structure of the polymeric outdoor insulator. Under uniformly wet-polluted conditions, the electric field intensity is less due to the wet layer covering the insulator surface and leading to a

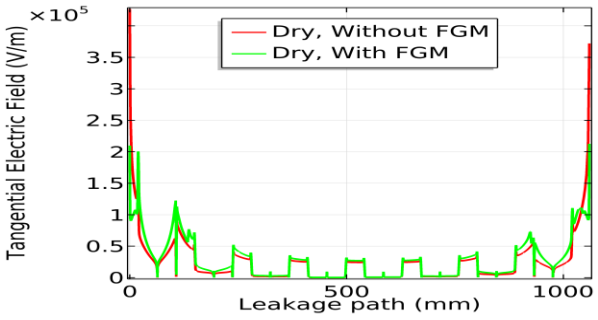

Fig. 5. The tangential field distribution along the insulator profile (clean-dry conditions)

more uniform electric field and equipotential lines distribution.

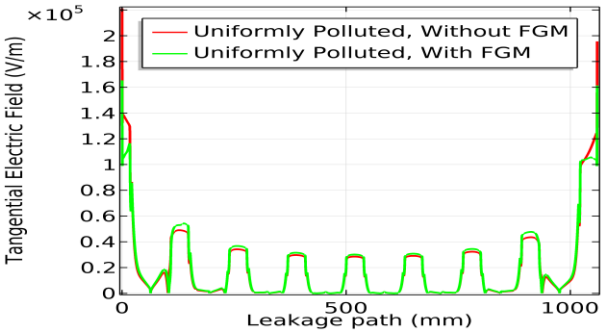

Fig. 6. The tangential field distribution along the insulator profile (uniformly wet-polluted conditons)

Adding field grading composite effectively decreases the electric field enhancements near both electrodes and offers more uniform field distribution. The non-linear field-dependent conductivity raises fast once the intensity of the electric field exceeds the field switching threshold, resulting in redistributing equipotential lines away from both electrodes and suppressing field enhancements at the triple junction. Fig. 7. shows the distribution of the equipotential lines near the HV terminal under different surface conditions without and with field grading composites having the optimized switching characteristics.

These encouraging results are expected to enhance the performance of the polymeric insulator, reduce the possibility of dry bands formation, and raise the flashover voltage by decreasing the probability of surface and corona discharges.

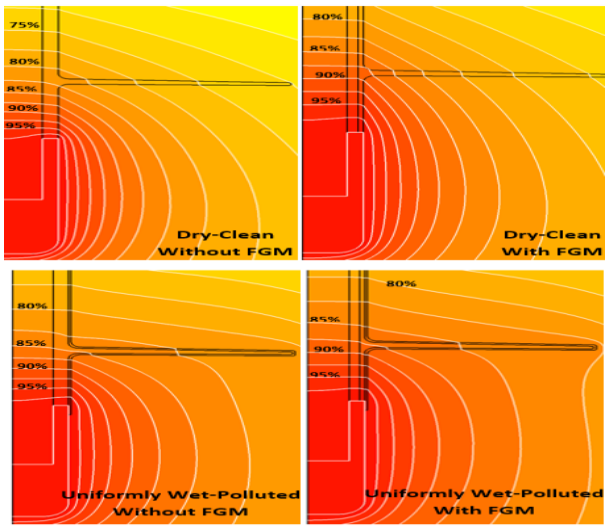

Fig. 7. The distribution of the equipotential lines near the HV terminal under dry and polluted conditions

4.2 Polymeric insulator performance with FGMs under polluted conditions with dry bands

Even though the electric field distribution is better under wet-polluted conditions, it represents the worst-case scenario. That is due to the electric field enhancements coupled with high current densities near both electrodes lead to uneven heating over the surface, resulting in dry bands formation. Fig. 8. shows the electric field distribution along the insulator profile with one dry band at the core region. The maximum electric field magnitude highly increased with the existence of the dry band compared with dry and uniformly wet-polluted. These dry bands magnify the electric field and consequently cause the initiation of intense arcs on the insulation surface and premature degradation of insulation materials. And under favorable conditions, it may lead to puncture the silicone housing and cause a complete flashover.

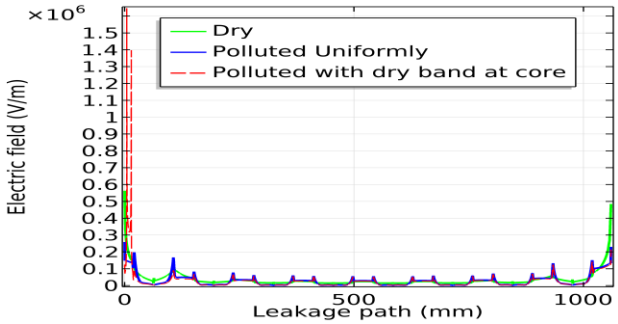

Fig. 8. The distribution of the electric field along the insulator profile

Fig. 9 shows the distribution of the electric field near the HV terminal with dry bands of 10 mm length formed at the core and the junction between the core and the shed without and with FGM. These dry bands greatly distort the electric field distribution, generate a large amount of heat, and initiate electric discharges on the

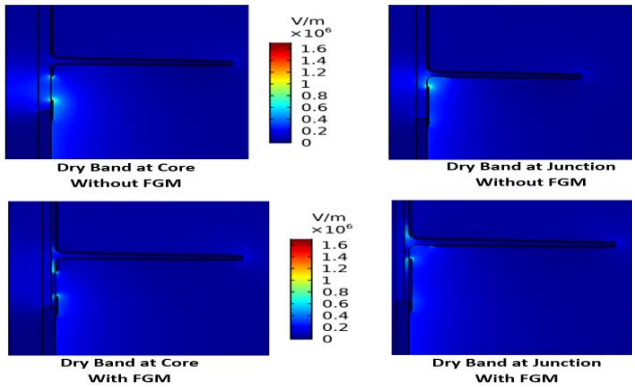

Fig. 9. The electric field distribution near the HV terminal with dry bands without and with FGM

insulator surface. The new insulator offers better performance with dry bands formation in different locations. That could be because of the more homogeneous distribution of electric fields and redistribute equipotential lines away from both terminals. In addition, the grading effect of non-linear FGM will raise with increasing the electric field intensity. The heat generated per unit volume along the insulator surface is computed and shown in Fig. 10 using equation [12]:

$$H_{gen} = \frac{E^2 \times \varepsilon_r \times f \times tan(\delta)}{1.8 \times 10^{12}}$$

Where E is the intensity of the electric field, $\varepsilon_r = 4.3$ is the relative permittivity of silicone rubber, $f = 50$ is the frequency, and $tan(\delta) = 0.006$ is the dissipation factor. As shown in Fig. 10, without FGM, the heat generated is too high near both terminals; hence, the prolonged extreme heating in this area is expected to form dry bands and consequently discharge activities. Using FGM reduces these peaks near the HV terminal by more than 37.5%, from 48 (mW/m^3) to 30 (mW/m^3). The insulator-equipped with field grading composite provide better performance compared with standard insulator. The electric field is lower and consequently lower heat generated. The simulation results demonstrate that the stress control of composite insulators using non-linear resistive field grading materials can offer a considerable enhancement under the pollution surface conditions by reducing both the electric enhancement and the heat generated.

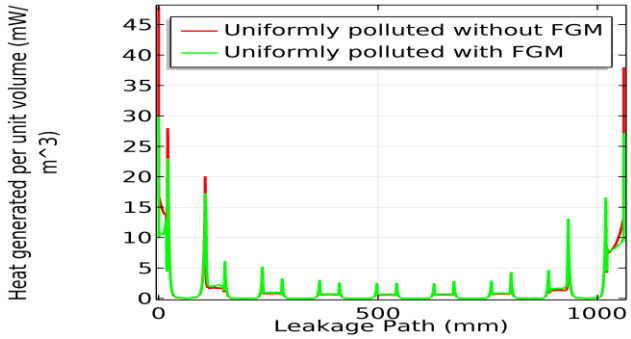

Fig. 10. The heat generated per unit volume along the insulator surface without and with FGM

4.3 Polymeric insulator performance with FGMs under dry conditions using 3D model

We developed the 3D model of the 33 kV polymeric insulator to consider the various structures that affect the distribution of electric fields and equipotential lines such as conductor and adjacent tower, obtaining a more accurate and realistic electric field distribution around the insulator. To overcome slow and intense numerical computations in 3D models and minimize calculation and processing time, we studied the effects of the conductor and the tower only near the insulator. The polymeric outdoor insulator without practical structures has a symmetrical electric field distribution along the leakage path, with a generally U-shaped profile. The presence of the attached hardware, such as conductors and towers, distorts the distribution of the electric field and equipotential lines.

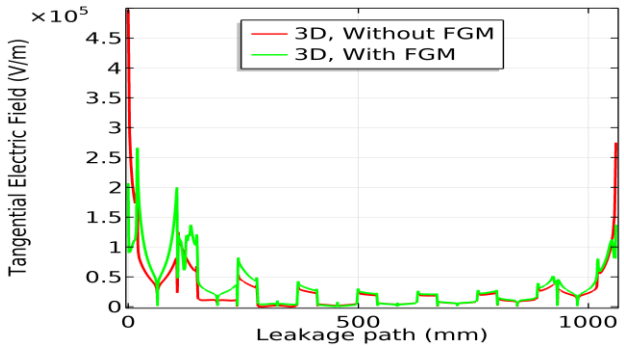

Fig. 11. The tangential field distribution along the insulator profile (clean-dry conditions)

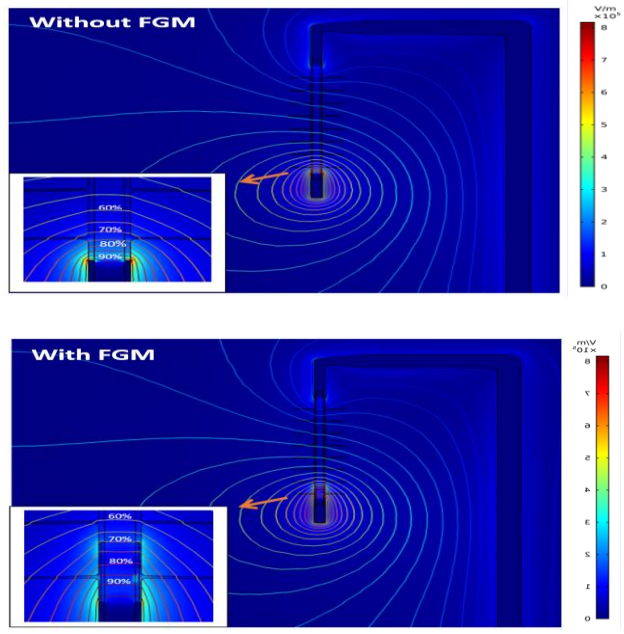

Fig. 12. The electric field and equipotential lines distribution of the 33 kV polymeric insulator

In contrast, field enhancements would be higher near the HV terminal due to the conductor effect. Fig. 11 shows the tangential electric field distribution along the insulator profile without and with FGM. Fig. 12 shows the electric field and equipotential lines distribution of the 33 kV composite insulators without and with FGM. Using

non-linear FGMs improves the distribution of the equipotential lines. Also, the insulator with non-linear field grading composites shows improved tangential electric field distribution, which agrees with the equipotential lines plot. The distribution of the tangential electric field is more homogeneous along the insulator profile, hence preventing extreme stress at vulnerable regions along the insulator surface (triple junction).

The maximum electric fields at the triple junction at both terminals are successfully decreased. Decrease from (6.8 to 4) kV/cm near the HV end-fitting and from (3.49 to 2.46) kV/cm near the GND end-fitting. Results show that the field reduction in the 3D model is more than in the 2D model because the higher electric field enhancements in 3D models would increase the gradient effect of field grading composites.

5. CONCLUSION

This paper studied the effect of non-linear resistive field grading composites for stress control of 33 kV polymeric outdoor insulators. The performance of the new polymeric insulator equipped with field grading composites based on ZnO microvaristors is evaluated using the Finite Element Method. Using 2D axisymmetric models, electric fields, equipotential lines distribution, and heat generated were computed and compared under various surface conditions (clean, uniformly wet-polluted, and with dry bands). A 3D model of the 33 kV polymeric insulator is developed to study the effect of practical structures such as the conductor and adjacent tower on the electric field, equipotential line distribution and obtain more accurate and realistic results. The proposed graded insulator shows improved electric field distribution with different surface conditions. The maximum electric field magnitude decreases under clean conditions from (5.63 to 3.66) kV/cm near the HV electrode, representing a 35% electric field reduction. Furthermore, the new proposed insulator reduces the maximum electric field and heat generated under uniformly polluted conditions by more than 20 % and 37%, respectively, while dry band formation at the core by more than 23 % and 37%, respectively, and with a dry band at the junction by more than 20% and 41%, respectively. The simulation results demonstrate that the field grading of polymeric outdoor insulators using non-linear resistive field grading composites can improve the insulator performance with different surface conditions. Hence, reduce the potential of dry bands formation and raise the flashover voltage. Further simulation and experimental work are planned for the actual insulators used in the field.

REFERENCE

[1] Hackam R. Outdoor HV composite polymeric insulators. IEEE Transactions on Dielectrics and Electrical Insulation, 6(5), 1999;557-585.

[2] Bonhôte P., Gmür T., Botsis J., & Papailiou K. O. Stress and damage analysis of composite–aluminium joints used in electrical insulators subject to traction and bending. Composite structures, 64(3-4), 2004;359-367.

[3] Tousi M. M., & Ghassemi M. Combined geometrical techniques and applying non-linear field dependent conductivity layers to address the high electric field stress issue in high voltage high-density wide bandgap power modules. IEEE Transactions on Dielectrics and Electrical Insulation, 27(1), 2021;305-313.

[4] Abd-Rahman R., Haddad A., Harid N., & Griffiths H. Stress control on polymeric outdoor insulators using zinc oxide microvaristor composites. IEEE Transactions on Dielectrics and Electrical Insulation, 19(2), 2012;705-713.

[5] Zhao X., Yang X., Hu J., Wang H., Yang H., Li Q., ... & Li X. Grading of electric field distribution of AC polymeric outdoor insulators using field grading material. IEEE Transactions on Dielectrics and Electrical Insulation, 26(4), 2019;1253-1260.

[6] Christen T., Donzel L., & Greuter F. Nonlinear resistive electric field grading part 1: Theory and simulation. IEEE Electrical Insulation Magazine, 26(6), 2010;47-59.

[7] Donzel L., Greuter F., & Christen T. Nonlinear resistive electric field grading Part 2: Materials and applications. IEEE Electrical Insulation Magazine, 27(2), 2011;18-29.

[8] Yang X., He J., & Hu J. Tailoring the non-linear conducting behavior of silicone composites by ZnO microvaristor fillers. Journal of Applied Polymer Science, 2015;132(40).

[9] Yang X., Zhao X., Hu J., & He J. Grading electric field in high voltage insulation using composite materials. IEEE Electrical Insulation Magazine, 34(1), 2018;15-25.

[10] Williams D. L., Haddad A., Rowlands A. R., Young H. M., & Waters R. T. Formation and characterization of dry bands in clean fog on polluted insulators. IEEE Transactions on Dielectrics and Electrical Insulation, 6(5), 1999;724-731.

[11] COMSOL Multiphysics, "User's Manual", Version 5.5, 2019.

[12] Nekahi A., McMeekin S. G., & Farzaneh M. Effect of pollution severity and dry band location on the flashover characteristics of silicone rubber surfaces. Electrical Engineering, 99(3), 2017;1053-1063.

